Iğdır Üniversitesi Fen Bilimleri Enstitüsü Dergisi, 13(3), 1676-1685, 2023
Journal of the Institute of Science and Technology, 13(3), 1676-1685, 2023

ISSN: 2146-0574, eISSN: 2536-4618

Physics **DOI: 10.21597/jist.1292270**

Research Article

Received: 04.05.2023 **Accepted: 13.06.2023**

To Cite: Levet, A. (2023). A Study of Photon İnteraction Parameters for Some Stainless Steel Alloys. *Journal of the Institute of Science and Technology*, 13(3), 1676-1685.

Aytaç LEVET*

A Study of Photon Interaction Parameters for Some Stainless Steel Alloys

Highlights:

- Radiation shielding parameters for stainless steels were determined
- Z_{eff} and N_{eff} strongly depend on the atomic numbers of the elements in the alloy.
- The interpolation and the direct methods were compared
- The radiation shielding capabilities of stainless steels were similar, and no considerable differences were found

ABSTRACT:

In this work, we investigated the effective atom number, the effective electron density, the mean free path, the tenth-value layer, the half-value layer, and the mass attenuation coefficient for some stainless steels: AISI 302, AISI 303, AISI 304, AISI 304L, AISI 310, AISI 316, AISI 321, and AISI 410. The mass attenuation coefficients were determined using the WinXCom computer program in the energy region 1keV- 100 GeV. The effective atom number and effective electron density have been calculated using two different methods, the direct method, and the interpolation method. The results reveal that the values of effective atomic numbers and effective electron numbers are greatly influenced by the atomic number of elements in the alloy and the interaction photon energy. The effective atom numbers grew as the atomic number of the constituents in the alloys increased. The effective atomic number and effective electron density values for all steels were found to have the highest values at 0–0.1 MeV energy and the lowest values in the 0.5–6 MeV energy range. The shielding properties of the steels produced close results, but AISI 304L provided the best protection while AISI 410 provided the least. The results obtained with both methods were also compared. The result of the present study may provide new and helpful knowledge about stainless steel for gamma-ray shielding applications.

Keywords:

- Radiation shielding
- Stainless steel
- Effective atomic number
- Effective electron density

Aytaç LEVET (Orcid ID: 0000-0002-1086-5732), Ataturk University, İspir Hamza Polat Vocational School, Department of Electricity and Energy, Erzurum, Türkiye

***Corresponding Author:** Aytaç LEVET, e-mail: aytaclevet@atauni.edu.tr

INTRODUCTION

Stainless steel alloys are widely used in many areas, such as engineering, nuclear, chemical, industry, aerospace, and medical industries (Marashdeh & Al-Hamarneh, 2021; Tekaslan et al., 2008). These alloys are critical in radiology and nuclear power plants where radiation is used extensively. Steel liner plates for the inner containment double-walled structure dome are utilized in modern reactor models for sealing under normal and accident conditions. The widespread use of carbon and stainless steel alloys in reactors and research projects necessitates the exploration of gamma-ray shielding qualities (Singh et al., 2015). The level to which gamma radiation decreases is determined by the incident gamma radiation's energy, the atomic number and density of the elements in the shielding substance, and the shielding thickness (McAlister, 2012).

Stainless steel grades consist of five primary grades. These are austenitic stainless, ferritic stainless, martensitic stainless, duplex stainless, and precipitation-hardening stainless steel (Gowthaman et al., 2020; Yontar, 2011). Austenitic stainless steels are the world's most widely used grade of stainless steel and are suitable for almost any environment (Kahraman et al., 2002). This class of materials does not harden by heat treatment, and these materials attract little or no magnets. On the other hand, austenitic stainless steels can undergo various structural transformations during cooling (de Bellefon et al., 2019). Martensitic stainless steels are generally the stainless steel grade used in applications where better mechanical strength is required, and this grade of stainless steel is more affordable than materials in the austenitic stainless steel grade. The most important feature of this stainless steel class, which generally holds magnets, is that heat treatment can be applied to stainless materials in this class. Martensitic stainless steels can be mechanically strengthened and hardened by heat treatment (Özer & Bahçeci, 2009; Szummer et al., 1999). Depending on the high carbon content, martensitic stainless steels containing 0.10% and above carbon elements can have a higher hardness. Ferritic stainless steel is a preferred stainless steel class because of its affordable cost, consisting of materials containing a minimum of 10.5% and above chromium, low carbon content, and little or no nickel element (Hu et al., 2020; Uyar, 2019). All ferritic stainless steel materials are magnetic and attract magnets. Materials in the duplex stainless steel class consist of a mixture of both ferritic and austenitic microstructures, and as a result of the combination of these two different internal structures, they are called duplex stainless. These materials, which contain both austenite and a ferritic phase in their metallurgical structures, are magnet-attracting and magnetic. Duplex stainless steels have better corrosion resistance than austenitic stainless steels, as well as better mechanical strength than austenitic stainless steels (Örnek et al., 2020). Precipitation-hardenable stainless steels are a class of stainless steel that can be hardened by heat treatment and further increase mechanical strength. This class of materials has similar corrosion-resistant properties as austenitic stainless materials. On the other hand, after precipitation hardening, this class of materials has very high mechanical strengths (Ludwigson & Hall, 1959). Standards have been established by different organizations for stainless steels. The American Iron and Steel Institute with the AISI code has determined the world's most widely used stainless steel standards. Our study has seven austenitic stainless steel samples and one martensitic stainless steel (AISI 410) sample.

Stainless steels are mainly iron-based alloys containing chromium and nickel. When the content of the chromium passivation membrane is high, stainless steel has a high degree of chemical stability and can generate a dense oxidizing medium toughness above 11.7% (Meng & Zhang, 2016). Ni, Mo, Mn, Si, Ti, and Nb elements are added in different proportions to give stainless steel different properties. Nickel increases the important properties of stainless steel such as weldability and ductility. Therefore, it is one of the most important components of stainless steel production. Molybdenum, found in small

amounts in stainless steel, can specifically harden at high temperatures. It also increases yield and tensile strength. Manganese increases the strength, hardenability, and weldability of steel. Silicon improves the high temperature resistance and magnetic properties of steel. In addition, it increases the tensile strength and elasticity of the steel, and it is generally used in spring steels that require high elasticity. Titanium and Niobium have a grain-reducing effect and strong carbide-forming properties and also increase the hardness of steel (Alım et al., 2022; Aygün, 2020). Work continues today on producing steel alloys using elements with different percentages to be used for appropriate purposes. It will continue to be used in many sectors for many years due to its price, robustness, neutron-catching ability, and production easiness. Table 1 shows the densities and contents of the stainless steels we discussed in this study.

Table 1. Density and chemical composition of stainless steels

Stainless Steels	Density (g/cm^3)	Elements (weight %)						
		Fe	Cr	Ni	Mn	Si	Mo	Ti
AISI 302	7.83	74	18	8	-	-	-	-
AISI 303	7.81	71	18	9	1	1	-	-
AISI 304	7.85	72	18	10	-	-	-	-
AISI 304L	7.99	72	10	18	-	-	-	-
AISI 310	7.91	55	25	20	-	-	-	-
AISI 316	7.92	69	18	10	-	-	3	-
AISI 321	7.81	72	18	9	-	-	-	1
AISI 410	7.78	87.5	12.5	-	-	-	-	-

The absorption, loss of energy, or scattering of gamma rays interacting with material depends on the substance's atomic number and density. We cannot mention a definite value for chemical compounds and alloys, although the atomic number is apparent for the elements. Because according to Hine who was the first person to introduce this notion, compounds, and alloys use the effective atomic number (Z_{eff}) (Hine, 1952). There are different methods in the literature to determine the effective atomic number. We used direct and interpolation methods to determine the effective atomic numbers of the alloys.

The mass attenuation coefficient (μ/ρ) is essential in finding the effective atomic numbers value and electron density. The mass attenuation coefficient (μ/ρ) is determined by using WinXcom, a computer program that gives (μ/ρ) values depending on the energy (in the energy region 1 keV-100 GeV) when quantities of compounds or alloys composed of elements with different ratios are entered (Gerward et al., 2004). Many studies exist for different materials in specific energy ranges related to radiation shielding and photon interaction parameters. The researchers have determined the effective atomic numbers value and effective electron density of some carbon steel (Singh et al., 2015), some saturated fatty acids (Kore et al., 2016), gold, bronze, and water matrixes (Esfandiari et al., 2014), some chemicals commonly used in the industry (Büyükyıldız, 2017; Levet & Özdemir, 2017; Raut et al., 2018), iron-boron alloys (Gan et al., 2021; Levet et al., 2020), and construction materials (Kiran et al., 2015; Toprak et al., 2023).

The effective atomic number and effective electron density are the primary parameters determining the material's radiation absorption rate. In this study, we determined the effective atomic number (Z_{eff}), effective electron density (N_{eff}), mean free path (MFP), tenth-value layer (TVL), half-value layer (HVL), and mass attenuation coefficient of stainless steel alloys (AISI 302, AISI 303, AISI 304, AISI 304L, AISI 310, AISI 316, AISI 321, AISI 410) using two different methods in the energy region from 1 keV to 100 MeV. Direct and interpolating are the most common and accurate methods for finding effective atomic numbers. The differences and similarities between these two methods were examined, and variation of Z_{eff}, N_{eff}, HVL, TVL, and MFP with photon energy was observed. This study was written to

compute the radiation parameters of stainless steel-containing materials used in most areas and to determine which energy ranges are more valuable.

MATERIALS AND METHODS

Photon Matter Interaction

The radiation intensity decreases exponentially when the gamma ray passes through the material. The reduction in intensity of a gamma-ray beam after passing through a solid of thickness t is represented as;

$$I(E) = I_0(E).e^{-\mu t} \quad (1)$$

where, μ is a linear attenuation coefficient described as absorption per unit thickness. It is generally more convenient to use the mass attenuation coefficient (μ/ρ); ρ (g/cm2) is the density of the absorber since the linear attenuation coefficient may vary due to the density variation concerning the physical state of the absorber. As a result, the previous equation can be written as

$$I(E) = I_0(E).e^{\left(\frac{\mu}{\rho}\right)t} \quad (2)$$

where I_0 is the first non-interacting beam emanating from the radiation source; I represents the gamma-ray beam after passing through the material; μ/ρ is the mass attenuation coefficient (cm^2/g), and t is sample mass thickness (g/cm^2).

Direct Method

The effective atomic number and effective electron density of chemical compounds and alloys have lately piqued the curiosity of researchers. Using the direct method, the molar fraction, atomic weight, atomic number, and mass attenuation coefficient of elements in the alloy were utilized to find the effective atomic number. The following formula can calculate Z_{eff} for alloys (Manohara et al., 2008),

$$Z_{eff} = \frac{\sum_i w_i A_i (\mu/\rho)_i}{\sum_j w_j \frac{A_j}{Z_j} (\mu/\rho)_j} \quad (3)$$

where w_i is the proportion by weight, A_i is the atomic weight, Z is the atomic number, and $(\mu/\rho)_i$ is the mass attenuation coefficient of the ith element calculated with WinXcom (Gerward et al., 2004).

Interpolation Method

The effective atomic number of compounds was calculated using the logarithmic interpolation procedure shown below (Singh et al., 2007):

$$Z_{eff} = \frac{Z_1(log\sigma_2 - log\sigma) + Z_2(log\sigma - log\sigma_1)}{log\sigma_2 - log\sigma_1} \quad (4)$$

where σ is the atomic cross-sections (barns/atom) of the alloy, σ_1 and σ_2, are the atomic cross-sections of the elements closest to σ ($\sigma_1 < \sigma < \sigma_2$). Z_1 and Z_2 are the atomic numbers of these elements. And the total atomic cross-section is calculated by dividing the compound's mass attenuation coefficient μ/ρ (cm2/g) by the total number of atoms contained in one gram of that alloy, as shown below:

$$\sigma_a = \frac{(\mu/\rho)_{comp}}{N_A \sum_i w_i/A_i} (barns/atom) \quad (5)$$

where $(\mu/\rho)_{comp}$ is the compound's mass attenuation coefficient, w_i is the fraction by weight of the element *i*, N_A is the Avogadro constant, and A_i is the atomic weight of the *i*th element. The effective

atomic number, Z_{eff}, has been calculated using the theoretical values of a compound's total atomic cross-section, σ_a.

Effective Electron Density (N_{eff})

Electron density is a measure of how likely it is to find an electron in a particular region of space. It refers to the number around an atomic nucleus or within molecular structures. The higher the concentration of electrons at a given point, the higher the electron density. Effective Electron density is denoted by N_{eff} and is formulated as

$$N_{eff} = N_A \frac{Z_{eff}}{[A]} \quad (6)$$

where Z_{eff} is the effective atomic number and $[A]$ is the mean atomic mass.

Mean Free Path, Tenth-Value Layer, and Half Value Layer

One of the critical parameters in radiation shielding is material thickness. Mean free path (MFP), tenth-value layer (TVL), and half-value layer (HVL) are the most used terms. The mean free path is the mean length a photon of known energy may travel through a substance without interacting. The thickness that halves the radiation intensity is called the half value layer (HVL). A material with one HVL thickness will attenuate 50% of the photons. Likewise, the thickness that decreases the radiation intensity to one-tenth is referred to as the "tenth value layer-TVL." The formulas of these terms are as follows,

$$\text{MFP} = \frac{1}{\mu} \quad (7)$$

$$\text{HVL} = \frac{\ln(2)}{\mu} \quad (8)$$

$$\text{TVL} = \frac{\ln(10)}{\mu} \quad (9)$$

RESULTS AND DISCUSSION

This study observed the energy-dependent change of the effective atomic number and the effective electron density of some stainless steels used in many fields. These results were determined using logarithmic interpolation and direct methods well-known in the literature. The effective atomic numbers for stainless steels are given in Figure 1. These values appear to change depending on the atomic number of the elements in stainless steel alloy. The most important factor determining the effective atomic number is the atomic number of the elements in the stainless steel alloy. It is seen in Figure 1.f) that AISI 316 steel has the highest effective atomic number among the steels we examined in this study. The high atomic number of molybdenum contained in AISI 316 steel has led to this result. It is also seen that the effective atomic number varies with energy. Photoelectric absorption, Compton scattering, and pair production dominate at particular energy intervals when the gamma-ray interacts with matter. It is seen that the maximum value of Z_{eff} is in the range of 1 keV – 0.1 MeV, and this depends on the dominance of the photoelectric absorption in this energy range. It is known that the photoelectric effect cross section increases in proportion to $Z^{4–5}$. Also, the cross-section of the photoelectric effect is reduced in proportion to the $E^{-3.5}$ of the photon energy. It is seen in the graphs that the Z_{eff} value is the minimum in the 0.5 – 6 MeV energy range. Compton scattering is dominant in this energy range, and the possibility of occurrence is related to the Z atom number. The pair production is predominant in energies greater than 6 MeV and is directly proportional to Z^2. It is seen in the graphs that the Z_{eff} value shows a slow-increasing tendency in the 5-100 MeV energy range, and it stays constant at higher energies.

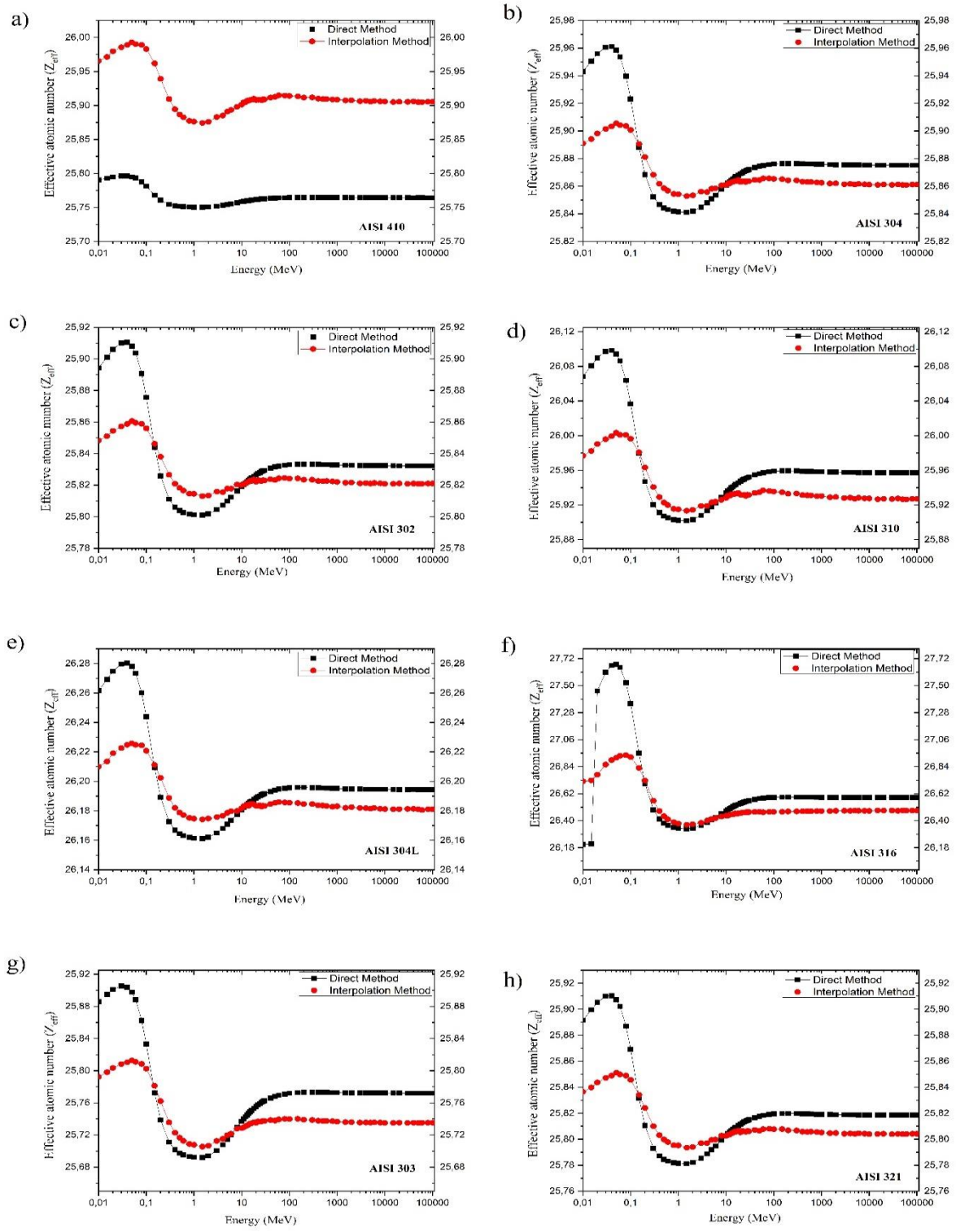

Figure 1. The relationship between effective atomic numbers and photon energy

The direct and interpolation methods we use to find the theoretical Z values in this work are two essential methods accepted in the literature. Z_{eff} values for all alloys are calculated using these methods and shown in the graphs. Although the study's methodologies produced broadly consistent results, some minor differences exist. It is seen that the interpolation method has higher values than the direct method in all energy ranges for only AISI 410 steel (Fig. 1.a). For all steels except AISI 410, Z_{eff} values calculated by the direct method are higher than those calculated by the interpolation method in the energy ranges where photoelectric absorption (1 keV – 0.1 MeV) and pair production (>6 MeV) dominate. On

the contrary, the Z_{eff} values calculated by the direct method are lower than those calculated by the interpolation method for the energy ranges in which Compton scattering (0.5 – 6 MeV) is dominant. It is seen that the methods give different results at different energies as the number of elements in the alloy grows.

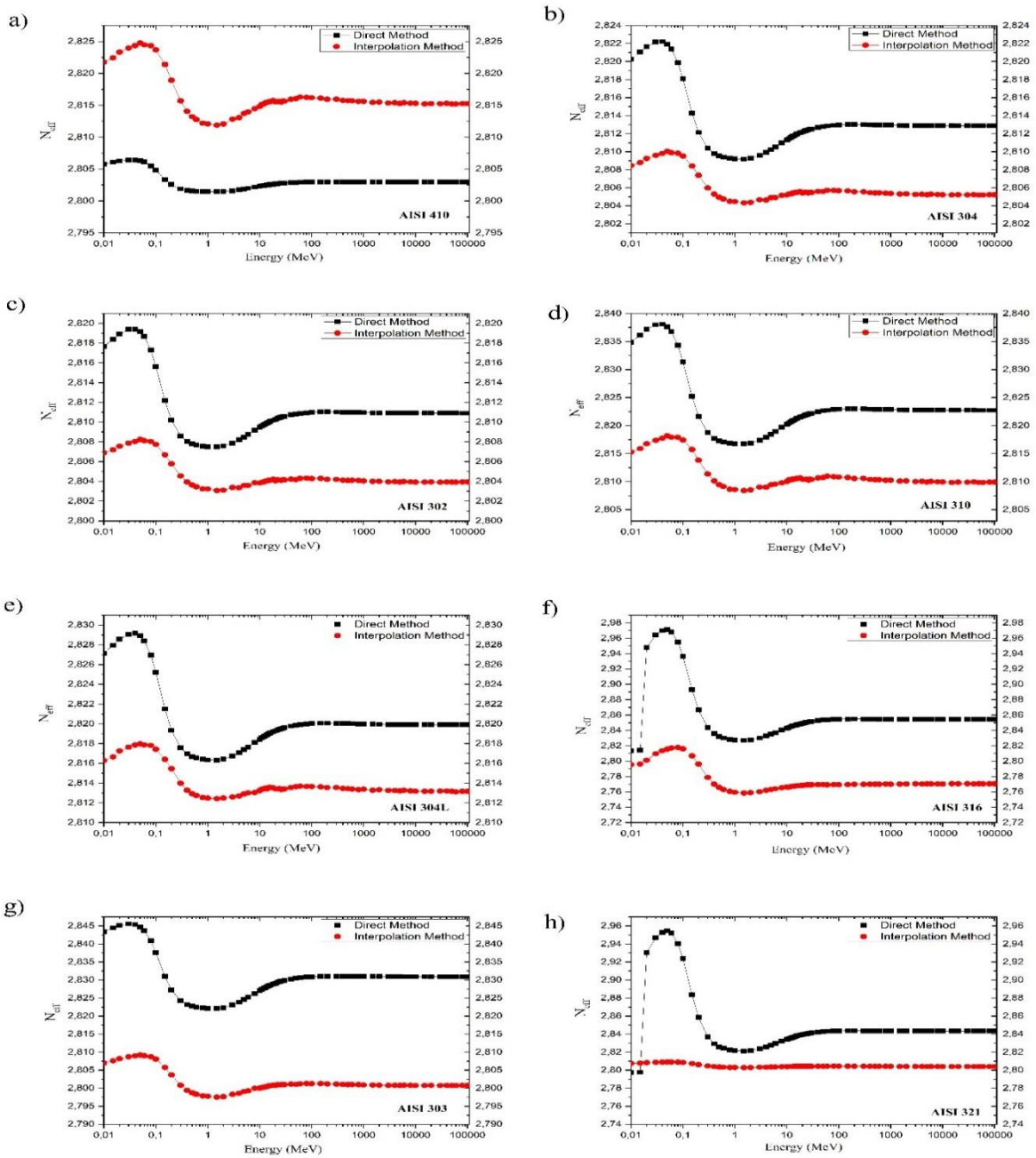

Figure 2. The relationship between effective electron density and photon energy

The effective electron density is also an important parameter used in radiation shielding. The effective electron densities obtained for stainless steels are given in Figure 2. Similar results were achieved because the effective electron density is directly correlated to the effective atomic number. Both methods produced similar outcomes. The data obtained by the interpolation method for only AISI 410 steel was higher than the data obtained by the direct method, as with the effective atomic number. However, unlike the data in Figure 1, there is a stable situation for all energy values. For example, while Z_{eff} values change direction in the 0.5–6 MeV energy range in Figure 1, this is not the case for N_{eff}. There

are deviations in some values seen in Figure 1. (f) and Figure 2. (f, h). This is thought to be because the alloying elements coincide with the absorption edges such as K and L.

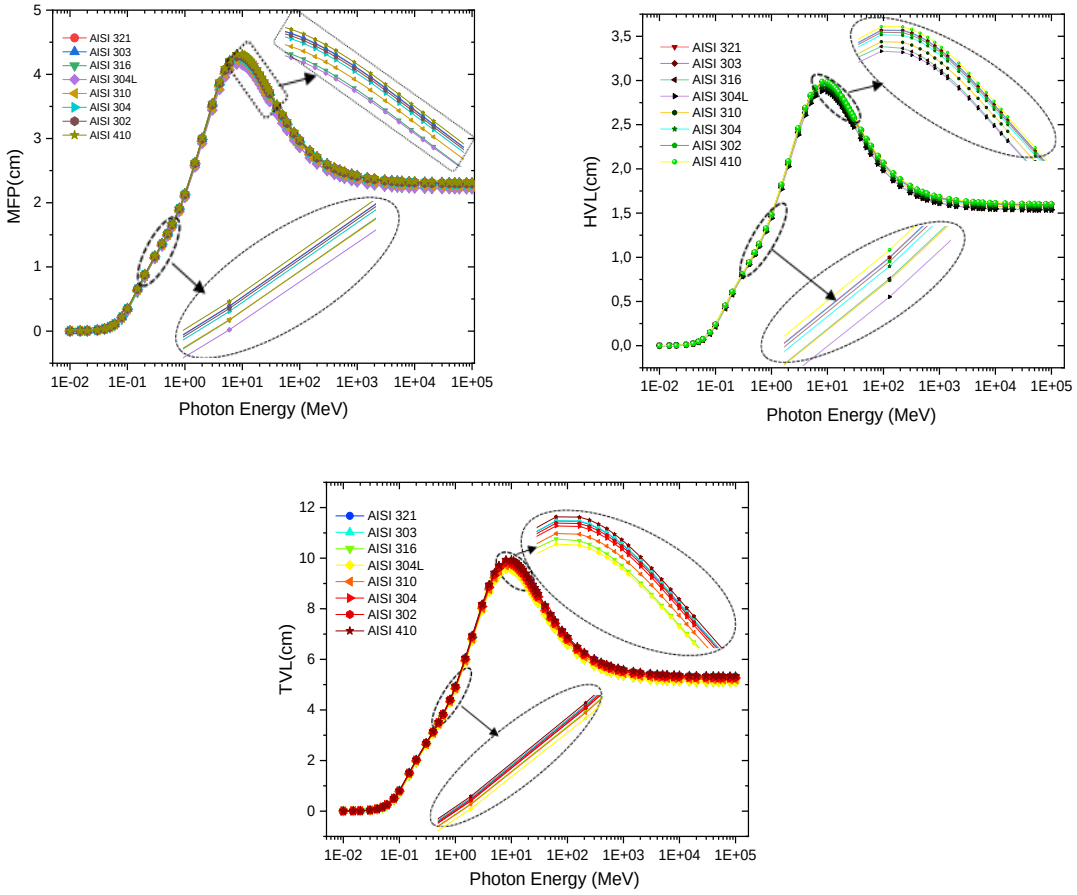

Figure 3. The relationship between HVL, TVL, MFP and photon energy

Figure 3. shows the HVL, TVL, and MFP values for stainless steels at 1 keV–100 GeV. We calculated the HVL, TVL, and MFP values to understand the radiation absorption performance of the materials. The smallness of these parameters is an essential factor in determining the materials to be used in radiation shielding. It can be seen from the graphs that the obtained values are close to each other. However, it is seen that AISI 304L has the lowest value, and AISI 410 stainless steel has the highest value. Thickness values in the energy range of 1 keV–100 keV have values below 1 cm. It increased linearly in the energy range of 100 keV–10 MeV. It is seen that HVL, MFP, and TVL values decrease exponentially after 10 MeV and remain constant after 1000 MeV.

CONCLUSION

In the present study, radiation shielding parameters have been established comparatively for stainless steels using two different methods in the energy region from 1 keV – 100 GeV. The energy dependent changes of the effective atomic number (Z_{eff}), effective electron density (N_{eff}), mean free path (MFP), tenth-value layer (TVL), and half-value layer (HVL) values for stainless steels have been calculated. The results of the study can be listed as follows:

- The atomic number of the constituent elements in the alloy has a major impact on the values of Z_{eff} and N_{eff}.

- Z_{eff} and N_{eff} values change depending on the energy and have the highest values at low energies, while they have the lowest values in the 0.5 – 6 MeV energy range.
- Interpolation and direct methods have produced similar results and agree with the experimental results in the literature (Gunoglu et al., 2021; Abdel-latif & Kassab, 2022).
- HVL, MFP, and TVL values are highest in the neighborhood of 10 MeV energy for all steels.
- Although the stainless steels investigated in this study have close parameters with minor differences (Mourad et al., 2021), AISI 304L steel showed the best performance. In addition, the order of shielding capabilities from best to worst is as follows: AISI 304L>AISI 316>AISI 310>AISI 304>AISI 302>AISI 321>AISI 303>AISI 410.
- It is clear that stainless steel can be a good radiation shield, especially for low-dose radiation applications.

Conflict of Interest

There is no conflict of interest.

REFERENCES

Abdel-latif M. A., & Kassab, M. M. (2022). Effect of chromium contents on radiation shielding and macroscopic cross-section in steel alloys. *Applied Radiation and Isotopes , 186*, 110263.

Alım, B., Özpolat, Ö. F., Şakar, E., Han, İ., Arslan, İ., Singh, V., & Demir, L. (2022). Precipitation-hardening stainless steels: Potential use radiation shielding materials. *Radiation Physics and Chemistry, 194*, 110009.

Aygün, B. (2020). High alloyed new stainless steel shielding material for gamma and fast neutron radiation. *Nuclear Engineering and Technology, 52*(3), 647-653.

Büyükyıldız, M. (2017). Calculation of effective atomic numbers and electron densities of different types of material for total photon interaction in the continuous energy region via different methods. *Sakarya University Journal of Science, 21*(3), 314-323.

de Bellefon, G. M., Robertson, I., Allen, T., van Duysen, J.-C., & Sridharan, K. (2019). Radiation-resistant nanotwinned austenitic stainless steel. *Scripta Materialia*, 159, 123-127.

Esfandiari, M., Shirmardi, S., & Medhat, M. (2014). Element analysis and calculation of the attenuation coefficients for gold, bronze and water matrixes using MCNP, WinXCom and experimental data. *Radiation Physics and Chemistry, 99*, 30-36.

Gan, B., Liu, S., He, Z., Chen, F., Niu, H., Cheng, J., . . . Yu, B. (2021). Research Progress of Metal-Based Shielding Materials for Neutron and Gamma Rays. *Acta Metallurgica Sinica, 34*(12), 1609-1617.

Gerward, L., Guilbert, N., Jensen, K. B., & Levring, H. (2004). WinXCom—a program for calculating X-ray attenuation coefficients. *Radiation Physics and Chemistry, 71*(3-4), 653-654.

Gowthaman, P., Jeyakumar, S., & Saravanan, B. (2020). Machinability and tool wear mechanism of Duplex stainless steel–A review. *Materials Today: Proceedings*, 26, 1423-1429.

Gunoglu, K., Özkavak, H. V., & Akkurt, İ. (2021). Evaluation of gamma ray attenuation properties of boron carbide (B4C) doped AISI 316 stainless steel: Experimental, XCOM and Phy-X/PSD database software. *Materials Today Communications, 29*, 102793.

Hine, G. J. (1952). The effective atomic numbers of materials for various gamma ray processes. *Phys. Rev., 85*, 725.

Hu, S., Mao, Y., Liu, X., Han, E.-H., & Hänninen, H. (2020). Intergranular corrosion behavior of low-chromium ferritic stainless steel without Cr-carbide precipitation after aging. *Corrosion Science*, 166, 108420.

Kahraman, N., Gülenç, B., & Akça, H. (2002). Ark kaynak yöntemi ile birleştirilen ostenitik paslanmaz çelik ile düşük karbonlu çeliğin mekanik özelliklerinin incelenmesi. *Gazi Üniversitesi Mühendislik Mimarlık Fakültesi Dergisi*, 17(2).

Kiran, K., Ravindraswami, K., Eshwarappa, K., & Somashekarappa, H. (2015). Effective atomic number of selected construction materials using gamma backscattering technique. *Annals of Nuclear Energy, 85*, 1077-1084.

Kore, P. S., Pawar, P. P., & Selvam, T. P. (2016). Evaluation of radiological data of some saturated fatty acids using gamma ray spectrometry. *Radiation Physics and Chemistry, 119*, 74-79.

Levet, A., Kavaz, E., & Özdemir, Y. (2020). An experimental study on the investigation of nuclear radiation shielding characteristics in iron-boron alloys. *Journal of Alloys and Compounds, 819*, 152946.

Levet, A., & Özdemir, Y. (2017). Determination of effective atomic numbers, effective electrons numbers, total atomic cross-sections and buildup factor of some compounds for different radiation sources. *Radiation Physics and Chemistry, 130*, 171-176.

Ludwigson, D., & Hall, A. (1959). *The physical metallurgy of precipitation-hardenable stainless steels*. Defense Metals Information Center, Battelle Memorial Institute, 111.

Manohara, S., Hanagodimath, S., Thind, K., & Gerward, L. (2008). On the effective atomic number and electron density: a comprehensive set of formulas for all types of materials and energies above 1 keV. *Nuclear Instruments and Methods in Physics Research Section B: Beam Interactions with Materials and Atoms, 266*(18), 3906-3912.

Marashdeh, M., & Al-Hamarneh, I. F. (2021). Evaluation of Gamma Radiation Properties of Four Types of Surgical Stainless Steel in the Energy Range of 17.50–25.29 keV. *Materials*, 14(22), 6873.

McAlister, R. D. (2012). Gamma ray attenuation properties of common shielding materials. *University Lane Lisle, USA*.

Meng, X. H., & Zhang, S. Y. (2016). *Application and development of stainless steel reinforced concrete structure.* Paper presented at the MATEC Web of Conferences.

Mourad, M., Saudi, H., Eissa, M., & Hassaan, M. 2021. Modified austenitic stainless-steel alloys for sheilding nuclear reactors. *Progress in Nuclear Energy*, 142, 104009.

Örnek, C., Larsson, A., Harlow, G. S., Zhang, F., Kroll, R., Carla, F., Hussain, H., Kivisäkk, U., Engelberg, D. L., & Lundgren, E. (2020). Metastable precursor structures in hydrogen-infused super duplex stainless steel microstructure–An operando diffraction experiment. *Corrosion Science*, 176, 109021.

Özer, A., & Bahçeci, E. (2009). Aisi 410 Martensitik Paslanmaz Çeliklerin Kesici Takim Ve Kaplamasina Bağli İşlenebilirliği. *Journal of the Faculty of Engineering & Architecture of Gazi University*, 24(4).

Raut, S., Awasarmol, V., Shaikh, S., Ghule, B., Ekar, S., Mane, R., & Pawar, P. (2018). Study of gamma ray energy absorption and exposure buildup factors for ferrites by geometric progression fitting method. *Radiation Effects and Defects in Solids, 173*(3-4), 329-338.

Singh, T., Kaur, P., & Singh, P. S. (2007). A study of photon interaction parameters in some commonly used solvents. *Journal of Radiological Protection, 27*(1), 79.

Singh, V. P., Medhat, M., & Shirmardi, S. (2015). Comparative studies on shielding properties of some steel alloys using Geant4, MCNP, WinXCOM and experimental results. *Radiation Physics and Chemistry, 106*, 255-260.

Szummer, A., Jezierska, E., & Lublińska, K. (1999). Hydrogen surface effects in ferritic stainless steels. *Journal of alloys and compounds*, 293, 356-360.

Tekaslan, Ö., Gerger, N., & Şeker, U. (2008). AISI 304 östenitik paslanmaz çeliklerde kesme parametrelerine bağlı olarak yüzey pürüzlülüklerinin araştırılması. *Balıkesir Üniversitesi Fen Bilimleri Enstitüsü Dergisi*, 10(2), 3-12.

Toprak, S. M. U., Polat, R., Levet, A., & Toprak, Ş. N. (2023). Effect of stone color, dosage and alkali type on Ahlat Stone (volcanic origin) based geopolymer concretes. *Journal of Building Engineering, 67*, 106059.

Uyar, M. 2019. *Borlanmış 430F ferritik paslanmaz çeliğin aşınma davranışı üzerine bir çalışma* (Yüksek lisans tezi). Fen Bilimleri Enstitüsü, https://acikbilim.yok.gov.tr/handle/20.500.12812/23541

Yontar, A. A. 2011. *AISI 304 paslanmaz çeliklerin işlenebilirliğinin incelenmesi*. (Yüksek Lisans Tezi), Selçuk Üniversitesi Fen Bilimleri Enstitüsü, Konya. https://tez.yok.gov.tr/UlusalTezMerkezi/tezDetay.jsp?id=Jda3vtcm-DIc039XxjY7yg&no=-A7T0aIh4ekAW_bq4pfCHA.